Our results suggest a new form of plasticity in that axons deprived of normal terminal sites, by the subtotal degeneration of cells in a target nucleus, shift their connections to local surviving neurons. Indeed, the hyperinnervation of selected neurons may itself play a role in determining which cells survive and which die.

E. HAZEL MURPHY
Department of Anatomy, Medical College of Pennsylvania, Philadelphia 19129

RONALD KALIL*
Department of Anatomy, University of Wisconsin, Madison 53706

References and Notes

1. K. L. Chow and J. H. Dewson III, *J. Comp. Neurol.* **128**, 63 (1966); D. Niimi and J. M. Sprague, *ibid.* **138**, 219 (1970); L. J. Garey and T. P. S. Powell, *Proc. R. Soc. London Ser. B* **169**, 107 (1967).
2. R. W. Doty, in *The Visual System: Neurophysiology and Psychophysics*, R. Jung and H. Kornhuber, Eds. (Springer, Berlin, 1961), p. 239; T. J. Tucker, A. Kling, D. P. Scharlock, *J. Neurophysiol.* **31**, 818 (1968); E. H. Murphy, R. R. Mize, P. B. Schechter, *Exp. Neurol.* **49**, 386 (1975).
3. R. E. Kalil, *Neurosci. Abstr.* **4**, 633 (1978).
4. R. W. Guillery, *J. Comp. Neurol.* **138**, 339 (1970); T. L. Hickey and R. W. Guillery, *ibid.* **156**, 239 (1974).
5. Since gyral patterns in the newborn kitten are poorly developed, we made large lesions to remove most of the cortex of the presumptive lateral, postlateral, and splenial gyri, but spared that of the suprasylvian gyrus. It is difficult to reconstruct precisely the extent of such large lesions made in neonatal brains because, during development, remaining adjacent cortical tissue is always disrupted and often assumes a bizarre configuration. We therefore estimated the size of each lesion on the basis of the severity and extent of retrograde degeneration in the LGN. In three of the five cats, the intended lesion was incomplete. One animal showed some surviving cells of all sizes throughout the LGN, and in two cats the rostral pole of the LGN was spared, although the rest of the nucleus was severely degenerated. The lateral geniculates in the two remaining cats were, with the exception of large surviving cells, completely degenerated, which indicates that the lesion in each case probably removed all of areas 17, 18, and 19. Cells recorded from these two cats represented about 65 percent of our sample and displayed the most striking abnormalities.
6. For details see R. R. Mize and E. H. Murphy, *J. Comp. Neurol.* **168**, 393 (1976).
7. P. O. Bishop, W. Burke, R. Davis, *J. Physiol. (London)* **162**, 451 (1962).
8. At the end of each experiment, the animal was perfused through the heart with 10 percent Formol-saline. The brain was blocked in the frontal plane and 40-μm frozen sections through the LGN and visual cortex were collected serially and stained with cresyl violet for cell bodies. Care was taken to locate each electrode track to ensure that all cells in our sample had been recorded from degenerated regions of the laminated part of the LGN and not from the medial interlaminar nucleus or the ventral lateral geniculate. Recording sites were identified by the location of small marking lesions that had been made with the microelectrode or by comparing the micrometer reading of each unit's depth below the cortical surface (as noted during the experiment) with measured distance along the reconstructed electrode track.
9. D. H. Hubel and T. N. Wiesel, *J. Physiol. (London)* **155**, 385 (1961). Some LGN cells have apparent excitatory or suppressive secondary surrounds outside the classic surround region [W. R. Levick, B. G. Cleland, M. W. Dubin, *Invest. Ophthalmol.* **11**, 302 (1972); L. Maffei and A. Fiorentini, *J. Neurophysiol.* **35**, 65 (1972); B. Dreher and K. J. Sanderson, *J. Physiol. (London)* **234**, 95 (1973); P. Hammond, *ibid.* **228**, 115 (1973)]. A small number of neurons located in the C layers of the LGN are atypical in having receptive fields that may be color-coded or nonconcentric [B. G. Cleland, W. R. Levick, R. Morstyn, H. G. Wagner, *J. Physiol. (London)* **255**, 299 (1976); P. D. Wilson, M. H. Rowe, J. Stone, *J. Neurophysiol.* **39**, 1193 (1976)].
10. J. Bullier and T. T. Norton, *J. Neurophysiol.* **42**, 244 (1979); P. D. Wilson *et al.*, in (*9*); B. Dreher and A. J. Sefton, *J. Comp. Neurol.* **183**, 47 (1979). In addition, our own control data from each cat provided further direct substantiation of the marked differences in receptive field size between cells in the normal and degenerated LGN.
11. P. O. Bishop, W. Kozak, W. R. Levick, G. J. Vakkur, *J. Physiol. (London)* **163**, 503 (1962); K. J. Sanderson and S. M. Sherman, *J. Neurophysiol.* **34**, 453 (1971); K. J. Sanderson, *J. Comp. Neurol.* **143**, 101 (1971).
12. Receptive fields of the five cells with wide-field sensitivity were mapped with a low-intensity stimulus to avoid an artifact resulting from stray light. Although it is not possible to exclude a relation between the wide-field responses we have observed and McIlwain's (*13*) periphery effect in normal LGN cells, our findings are clearly different. When contrast outside of the receptive field is varied by local stimulus movement, cells showing the periphery effect display a lowered threshold to center stimulation or a gradual increase in maintained discharge, but, in contrast to our results, they do not give direct, sharply timed responses to the peripheral stimulus [B. G. Cleland, M. W. Dubin, W. R. Levick, *J. Physiol. (London)* **217**, 473 (1971); B. G. Cleland *et al.*, in (*9*)].
13. J. T. McIlwain, *J. Neurophysiol.* **27**, 1154 (1964).
14. J. D. Daniels, J. D. Pettigrew, J. L. Norman, *ibid.* **41**, 1373 (1978).
15. This view is strengthened by anatomical studies of the retinogeniculate pathway in cats operated on as infants (*3*), which show that axons from the retina often run orthogonal to the lines of projection in the LGN and form exceptionally dense terminal fields in the immediate vicinity of large surviving neurons.
16. For review, see R. D. Lund, *Development and Plasticity of the Brain* (Oxford Univ. Press, New York, 1978).
17. Supported by NIH grants EY01331 (R.K.) and EY01122 and EY02488 (E.H.M.). We thank R. W. Guillery and P. D. Spear for helpful comments.
* Present address: Department of Ophthalmology, University of Wisconsin, Madison 53706.

9 July 1979; revised 31 August 1979

Molecular Microanalysis of Pathological Specimens in situ with a Laser-Raman Microprobe

Abstract. *A laser-Raman microprobe has been used to identify microscopic inclusions of silicone polymer in standard paraffin sections of lymph node. This example of organic chemical microanalysis in situ in pathological tissue represents an extension of microanalytical capabilities from elemental analysis, performed with electron and ion microprobes, to compound-specific molecular microanalysis.*

We report here the successful application of micro-Raman spectroscopy to the detection and identification of complex silicone polymer fragments in standard tissue sections. This technique, developed recently in two laboratories (*1*, *2*), offers exciting new prospects for biological studies by providing nondestructive compound-specific molecular microanalysis with good spatial resolution and high sensitivity to principal molecular components. A major weakness of current techniques [employing electron (*3*), proton (*4*), and ion (*5*) beam instruments with x-ray or secondary ion analysis] has been their general limitation to inorganic and elemental rather than organic and compound identification.

The instrument we used, which was developed at the National Bureau of

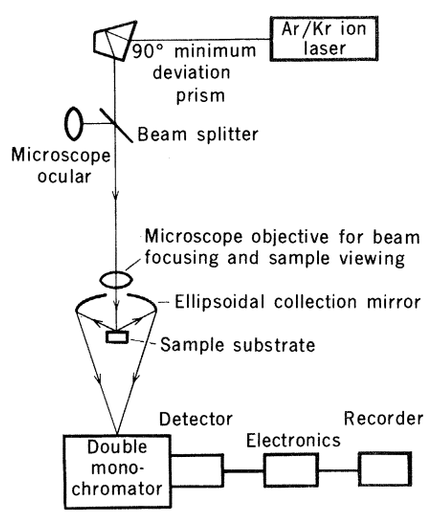

Fig. 1. Schematic diagram of the laser-Raman microprobe developed at the National Bureau of Standards. Any one of several laser wavelengths in the visible region of the spectrum is used to excite the micro-Raman spectrum. Nonlasing plasma lines are removed by use of a predispersing prism. The radiation scattered by the sample is collected over a large solid angle in 180° backscattering geometry. Lateral spatial resolution of the probe measurement is determined by the spot size of the laser on the sample and a spatial filter (exit pinhole, not shown) placed in the path of the collected scattered light. Depth resolution is several micrometers (but less than ~ 12 μm), depending on the optical transparency and surface topography of the sample. Typical measurement parameters employed in the microanalysis of thin sections of biological soft tissue are: laser wavelength, 514.5 nm (green) and 647.1 nm (red); laser power, 5 to 60 mW (at sample); laser spot diameter, 6 to 20 μm; time constant, 1 to 5 seconds; scan rate, 50 to 10 cm^{-1} per minute; and spectral slit width, 3 cm^{-1}.

0036-8075/79/1109-0716$00.50/0

Standards, is shown schematically in Fig. 1 and has been described in detail elsewhere (*2*). So far, it has principally been used for the identification and spectroscopic characterization of individual microscopic particles in various types of environmental samples (*6, 7*). The microprobe is basically a conventional monochannel Raman spectrometer, optimized to permit the acquisition of analytical-quality spectra from single microparticles or sample regions of micrometer dimensions.

In order to elicit Raman scattering ing from the microsample, the light beam from an argon-krypton ion laser is focused to a small spot (typically 2 to 20 μm in diameter) on the sample, and the scattered radiation—efficiently collected by an ellipsoidal mirror—is transferred into a double monochromator equipped with holographic gratings. The signal is detected by a cooled photomultiplier tube and processed by photon counting electronics. The sample, in this study a thin section of biological tissue a few millimeters in lateral dimensions, is supported by a substrate that does not give rise to troublesome spectral interferences. Single-crystal sapphire (α-Al_2O_3) of optical quality serves as a good substrate material. It is chemically inert, transparent to the exciting radiation (and hence does not heat), and free from laser-induced fluorescence in the spectral range of interest. Although sapphire has a Raman spectrum of its own, even the few predominant bands are relatively weak in intensity and do not seriously interfere with the spectra of unknowns.

The spectra obtained with the Raman microprobe are the so-called Stokes-Raman spectra (*8*) and are recorded as plots of scattered light (photon) intensity versus Raman shift. The lines or bands in a spectrum arise from molecules that scatter photons of lower frequency (Stokes lines) than the exciting line. The displacements of the Raman lines from the exciting line are identified with the frequencies of molecular vibration in the sample. Thus these spectra of the Raman-scattered light identify the scattering molecules and, in the case of solid samples, contain additional information on the molecular order of the solid phase from which the nature and extent of crystallinity may be inferred. The observed micro-Raman spectra have been shown to be identical to or, in some cases, even more detailed and informative than the corresponding bulk Raman spectra obtained from macroscopic samples (crystals or powders) of the same materials (*1, 2, 6, 7*).

For measurements to be successful in the Raman microprobe, the sample cannot be highly absorbing at the exciting laser wavelength. Appreciable absorption of the intense incident radiation invariably leads to sample heating or destruction, even though good thermal contact with the substrate may provide some degree of heat dissipation. Initially there was some concern that biological samples would be quickly burned under the intense irradiation, which may reach several thousand watts per square centimeter. This has not proved to be the case, and many sections of tissue conventionally prepared have been stable enough under the beam to yield satisfactory Raman spectra.

In this study we used the 514.5-nm (green) line of the laser to obtain the spectra of interest; the laser irradiance (power per unit area) was in the range 2 to 20 kW/cm^2. In other investigations of hard tissue (such as bone and tooth) laser light with irradiance levels as high as 0.2 MW/cm^2 was focused on the specimen

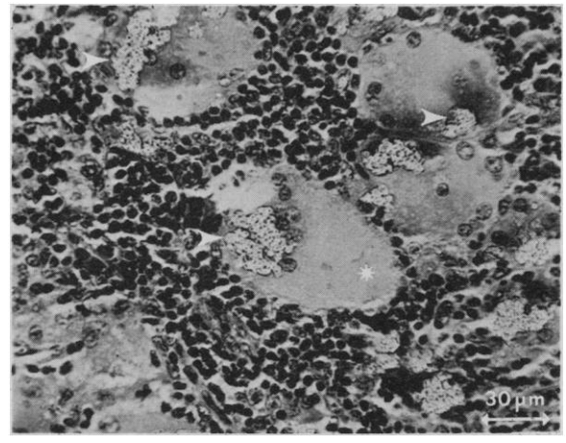

Fig. 2. Standard (5-μm) section of lymph node with foreign bodies of silicone rubber within multinucleated giant cells. Photomicrograph, in transmitted light, hematoxylin and eosin stain. Arrowheads indicate several typical inclusions of silicone polymer. Asterisk shows cytoplasmic area analyzed to obtain the micro-Raman spectrum of the host tissue matrix.

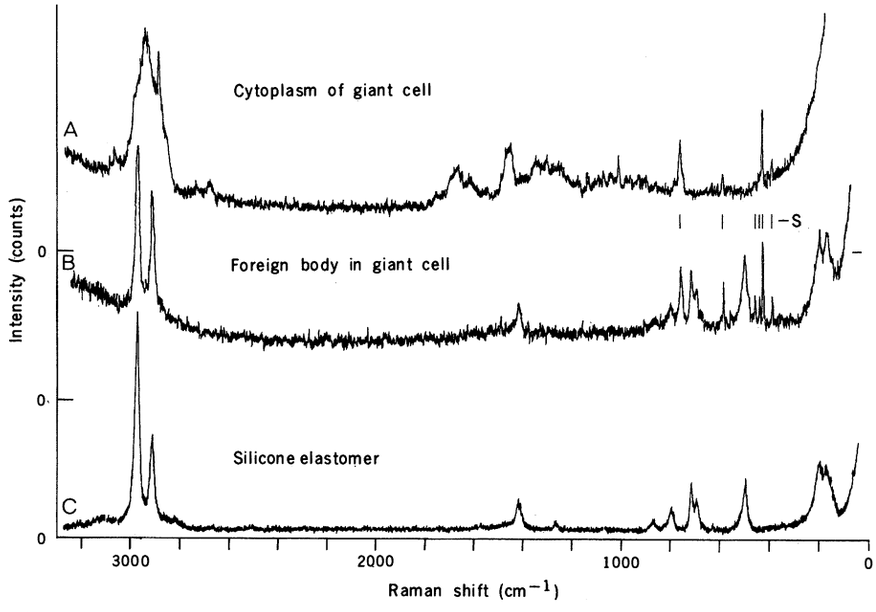

Fig. 3. Spectra recorded in the Raman probe microanalysis of a deparaffinized standard 5-μm section of lymph node (Fig. 2), mounted on a sapphire (α-Al_2O_3) substrate. Measurement parameters common to each spectrum are; excitation, 514.5 nm; laser spot diameter, 16 μm; exit pinhole spatial filter, 140 μm in diameter; and spectral slit width, 3 cm^{-1}. (A) Spectrum of the cytoplasm away from foreign bodies. Laser power was 40 mW (at sample); time constant, 5.0 seconds; and scan rate, 20 cm^{-1} per minute. (B) Spectrum of a foreign body (size ~ 24 μm) located within a giant cell. Measurement conditions were the same as for (A). (C) Spectrum of a small (~ 60 μm) particle of silicone elastomer from a joint prosthesis. Laser power was 60 mW (at sample); time constant, 0.5 second; and scan rate, 100 cm^{-1} per minute. The bands marked *S* on spectra (A) and (B) are contributed by the sapphire substrate. The vertical scale (scattered light intensity) of each spectrum extends from 0 to 1000 counts, with the strongest peaks at ~ 3000 cm^{-1} having nearly full-scale intensity. Zero intensity is indicated for each spectrum, allowing differences in background signal levels to be noted (see text).

without deleterious effects. Furthermore, potential fluorescence interferences from major or minor components of the sample analyzed under these conditions have not been a limitation. In other studies with longer-wavelength radiation (647.1 nm; red), the spectra obtained had fluorescent background levels significantly smaller than those encountered in spectra excited with 514.5-nm radiation. When fluorescence (or emission by the sample of other forms of non-Raman light) is observed in microprobe spectra, its origin is not always easily traced.

For this work we used a standard paraffin block of a formaldehyde-fixed biopsy of an enlarged axillary lymph node from a patient with a silicone elastomer finger-joint prosthesis (*9*). Standard 5-μm sections were prepared for initial examination by light microscopy (glass slides), scanning electron microscopy (SEM), and energy-dispersive x-ray microanalysis (EDXA) (carbon disks). Parallel sections (unstained) were mounted on sapphire sample supports and deparaffinized with xylene for subsequent Raman microprobe analysis. The light micrograph of a stained section of the lymph node shown in Fig. 2 demonstrates the foreign material within multinucleated giant cells. The SEM and EDXA analyses (performed by J.L.A.) proved that the foreign bodies contained silicon. This suggested that the microscopic fragments were silicone rubber particles from the prosthesis, but direct molecular identification was not possible with the information furnished by the x-ray spectrum. The material did not resemble any inorganic crystalline or glassy structure under the light microscope or SEM optics. The histology of the unstained sample section on the sapphire substrate was recognizable in the optics of the laser-Raman system. The beam was placed on areas of tissue away from the inclusions of foreign material and spectra were obtained (Fig. 3). Spectra were then obtained from 12 individual inclusions, which showed identical and characteristic peaks at several wavenumbers. These were compared with spectra obtained under the same conditions from particles abraded directly from a new silicone rubber joint prosthesis. The spectra of the inclusions in the giant cells contained peaks identical to those in the spectra of the prosthesis, plus additional peaks attributable to the tissue matrix. The micro-Raman spectrum of the prosthesis was identical to published bulk Raman spectra of polydimethyl siloxane (*10*).

A similar sample preparation technique may be satisfactory for analysis of many heretofore unidentifiable materials in tissues. Special techniques such as cryosectioning and freeze-drying (*11*) or embedding in other media may be necessary to prevent loss or alterations of certain materials (*12*). Some media, such as epoxy and methacrylate resin, have interfering Raman spectral emissions. By using computer methods to strip out the spectral component arising from the embedding material, one can obtain a useful spectrum that is more easily interpreted. Further research is needed on the critical aspects of sample preparation and handling and their effect on the micro-Raman measurement. We would expect that the less material from the embedding or processing that remains, the more straightforward the resulting analysis will be.

Limitations of this kind of analysis are due to the signal-to-noise ratio of the instrumentation and the light optics of the laser system. Currently, the smallest spot size is on the order of 1 μm. The sensitivity (detection limits) of this system depends on several variables, including the instrument design, the volume analyzed, the Raman scattering cross section (Raman scattering efficiency) of the compound of interest in a given matrix, and the distribution of the Raman scatterer (compound of interest) in the sample matrix. Work is being done to better define the sensitivity to major and minor components in various matrices. For example, Blaha *et al.* (*7*) estimated that carbon coating on environmental particles has been detected at levels of less than 1 percent by weight (in the picogram range by absolute mass detected). Improved optics and signal processing techniques can be expected to increase the efficiency of the system in new instrumentation.

It is important in studying tissues for diagnostic or forensic applications to be able to correlate the analysis with the morphology. In situ microanalysis may often be much more valuable than bulk analysis, which destroys topographic relationships. In this way, materials associated with specific pathological reactions can be identified (*3*). We believe that this laser-Raman microprobe system, by extending microanalytical techniques from the elemental to the molecular level, has a great potential for use in many applications in pathology, toxicology, forensics, and environmental studies.

JERROLD L. ABRAHAM
Department of Pathology, University of California at San Diego, La Jolla 92093

EDGAR S. ETZ
National Measurement Laboratory, Center for Analytical Chemistry, National Bureau of Standards, Washington, D.C. 20234

References and Notes

1. M. Delhaye and P. Dhamelincourt, *J. Raman Spectrosc.* **3**, 33 (1975); P. Dhamelincourt, F. Wallart, M. Leclercq, A. T. N'Guyen, D. O. Landon, *Anal. Chem.* **51**, 414A (1979).
2. G. J. Rosasco, E. S. Etz, W. A. Cassatt, *Appl. Spectrosc.* **29**, 396 (1975); G. J. Rosasco and E. S. Etz, *Res. Dev.* **28**, 20 (1977).
3. J. L. Abraham, in *The Lung*, W. T. Thurlbeck, Ed. (Williams & Wilkins, Baltimore, 1978), pp. 96–137; J. L. Abraham, in *Scanning Electron Microscopy/1979/II* (IIT Research Institute, Chicago, 1979), p. 751.
4. P. Horowitz, M. Aronson, L. Grodzins, W. Ladd, J. Ryan, G. Merriam, C. Lechene, *Science* **194**, 1162 (1976).
5. J. L. Abraham, R. Rossi, N. Marquez, R. M. Wagner, in *Scanning Electron Microscopy/1976/I* (IIT Research Institute, Chicago, 1976), p. 501; M. B. Bellhorn and R. K. Lewis, *Exp. Eye Res.* **22**, 505 (1976); A. W. Szanderna, A. C. Miller, H. F. Helbig, in *Scanning Electron Microscopy/1978/I* (ITT Research Institute, Chicago, 1978), p. 259.
6. E. S. Etz, G. J. Rosasco, J. J. Blaha, in *Environmental Pollutants*, T. Y. Toribara, J. R. Coleman, B. E. Dahneke, I. Feldman, Eds. (Plenum, New York, 1978), pp. 413–456; J. J. Blaha and G. J. Rosasco, *Anal. Chem.* **50**, 892 (1978).
7. J. J. Blaha, G. J. Rosasco, E. S. Etz, *Appl. Spectrosc.* **32**, 292 (1978).
8. Observed in the microprobe is the normal or spontaneous Raman effect. This effect is the basis for conventional Raman spectroscopy and has been reviewed in the context of modern chemical analysis [see, for example, D. E. Irish and H. Chen, *Appl. Spectrosc.* **25**, 1 (1971); A. C. Eckbreth, P. A. Bonczyk, J. F. Verdieck, *Appl. Spectrosc. Rev.* **13**, 15 (1978)]. Raman spectroscopy in the biological sciences has been reviewed by N.-T. Yu [*Crit. Rev. Biochem.* **4**, 229 (1977)].
9. A. J. Christie, K. A. Weinberger, M. Dietrich, *J. Am. Med. Assoc.* **237**, 1463 (1977).
10. J. Maxfield and I. W. Shepherd, *Chem. Phys.* **2**, 433 (1973).
11. P. Echlin and A. J. Saubermann, in *Scanning Electron Microscopy/1977/I* (IIT Research Institute, Chicago, 1977), p. 621.
12. M. G. Wickham, R. Rudolph, J. L. Abraham, *Science* **199**, 437 (1978).
13. We thank A. Christie for providing the tissue sample. Supported in part by PHS grant HL 19619.

26 June 1979